

## **EFFECT OF PIP2 ON VESICLES RELEASE IN NEURAL CELLS**

2021-09-13 – 2022-01-17  
Version 2

Bachelor Thesis Project in Biomedicine  
30 ECTS  
Autumn term/Spring term Year

**Author:**

Jonathan Wahlund – e18jonwa@student.his.se

**Supervisors:**

Nikhil R. Gandasi – nikhil.gandasi@mcb.uu.se  
University of Gothenburg, Unit of Metabolic Physiology at  
Department of Neuroscience and Physiology  
Medicinaregatan 11, 413 90 Gothenburg

Amir Hatamie – amir.hatami@gu.se  
University of Gothenburg, Department of Chemistry and  
Molecular Biology  
Kemigården 4, 412 58 Gothenburg

**Co-supervisor:**

Katarina Ejeskär – katarina.ejeskär@his.se  
University of Skövde, Institution of Health Sciences  
Högskolevägen 1, 541 28 Skövde

**Examiner:**

Ferenc Szekeres – ferenc.szekeres@his.se  
University of Skövde, Institution of Health Sciences  
Högskolevägen 1, 541 28 Skövde

## Contents

Introduction.....	1
Materials and methods .....	2
Imaging – Confocal.....	2
PC12 Cells .....	2
Plasmids and Solutions.....	2
Microscopy .....	3
Image Analysis.....	3
Statistics .....	3
Amperometric Analysis .....	3
Bovine Chromaffin Cell.....	3
Vesicle Isolation.....	3
Addition of PIP2.....	4
Carbon Fiber Electrode Fabrication.....	4
Vesicle Impact Electrochemical Cytometry.....	4
Amperometric Analysis .....	4
Statistics .....	5
Results .....	5
Imaging Results .....	5
Vesicle Impact Electrochemical Cytometry Results.....	9
Discussion.....	11
Acknowledgments.....	12
Reference .....	13

## Abstract

Lipids serve numerous different processes in biological cell communication. As for the case of Phosphatidylinositol-(4,5)-biphosphate (PIP2), which serves actin-dynamics, endocytosis, and of recent importance, exocytosis. PIP2 proceeds these functions at the cell's plasma membrane, which yields the possibility to also exist at the membrane of large dense-core vesicles. With the lipids functions previously known, what factor does PIP2 serve if located on the membrane? This study intends to use confocal imaging and vesicle impact electrochemical cytometry to study the location and function respectably of the lipid membrane. Analysis was carried out on both PC12 cells as cell line and bovine chromaffin as primary cells for each respective analysis. Phospholipase C delta-1 (PLC $\delta$ 1) markers were used in the microscopy experiments. The external application of PIP2 on extracted large dense-core vesicles (LDCV) experimentally was performed. This study observed the location of PIP2 is indeed on large dense-core vesicles well apart from the plasma membrane. In the extracted large dense-core vesicles which was used a model to study how the changes in PIP2 levels affect fusion, increasing PIP2 levels significantly reduced the half-time of LDCV. Indicating that PIP2 effect is on the membrane stability, resulting in rapid breakup of LDCV membrane. Which is probably resulted by affecting membrane order from clustering PIP2. These findings broaden our understanding of the lipid PIP2, as it also lay way for future research, among cell-to-cell communication, vesicles, and hormonal treatment. It also indicates the useability of combining imaging and amperometric for observational studies.

## Introduction

An unimaginably complex network of cells makes up the human body. These cells carry their shape and functions with the primary purpose of continuous survival. To serve their design, they must appropriately react to external and internal changes in their surroundings. With cell-to-cell communication, these cells can propagate befitting responses to current changing circumstances in their environment. Although the cells have numerous different ways to communicate, the use of neurons allows the combination of both electrical and chemical signalling. These neurons exist in the central and peripheral nervous systems and handle receiving, processing, and moving forward messages. This specific type of messaging is very efficient when regarding distance and strength of the message as a factor. For example, in this thesis, the splanchnic nerve, when activated, stimulates the medulla area of the adrenal gland, causing a release of neurotransmitters from the Chromaffin cells—primarily releasing neurotransmitters such as norepinephrine and epinephrine through exocytosis—acting on responses to stress and fight-or-flight response respectively.

Chromaffin cells with their large-dense core vesicles (LDCV) have been a traditional cell to culture with the intent to study parts and factors correlated with exocytosis, cell communication, and vesicles (Westerink & Ewing., 2008; Bader et al., 2002; Chen et al., 1994). The most used kind of these cells is either PC12 or fresh bovine samples for each befitting analysis (Westerink & Ewing., 2008; Bader et al., 2002; Greene & Tischler., 1976). These cells have been used extensively to analyse the lipid phosphatidylinositol (4,5) bisphosphate (PIP<sub>2</sub>), a major cell-to-cell communication factor (Mandal., 2020; Kabachinski et al., 2014; Bader et al., 2002). PIP<sub>2</sub> has a part in many different functions, propagated by forming nanodomains at the plasma membrane (PM), given rising due to lipids' chemical structure, which consists of a large headgroup and multivalent negative charge. A charge serves as an interacting centre for multiple different molecular entities (Bilkova et al., 2017; Sarmiento et al., 2014). PIP<sub>2</sub> is enriched at the cell plasma membranes in which it consists of high-concentrated nanodomains, created due to the ability to cross-link with other molecules of itself (Bilkova et al., 2017; Sarmiento et al., 2014). These nanodomains allow the binding of proteins to the plasma membrane, in which, depending on the binding molecule, functions such as actin-dynamics, endocytosis, and exocytosis can be exercised (Mandal., 2020; Tuosto et al., 2015; Martin., 2012; Grishanin et al., 2004; Hay et al., 1995). Even if extensively analysed, much uncertainty exists around precise location and functions especially its part in exocytosis.

A method to analyse cell-to-cell communication factors is with Amperometry, as any electroactive molecule can change the current yielding an analytical result. Both previously mentioned neurotransmitters are electroactive, oxidizing in contact with positive potential. The change in current occurs when an electrode with positive potential is held near electroactive molecules. Which increases until the vesicle is out of neurotransmitters to oxidize. The changing current grants observation using Faraday's law to calculate the number of molecules through a peak representing the oxidated neurotransmitters. Early use of this method consisted of having the electrode near the cell and awaiting vesicles' release or even lysing them to acquire the vesicles. The Ewing group manifested a technique to directly isolate vesicles and place the polarised electrode in a suspension containing pure vesicles, to acquire yields from vesicles (Chen et al., 1994). The yields acquired from the bursting of

pure vesicles show clear peaks to be analysed. This method, "Vesicle Impact Electrochemical Cytometry" (VIEC), allows analysis of vesicle fusion kinetics.

Although, data from electrochemical methods is limited from capture a broader picture of cellular processes/function at a fundamental level. VIEC does not explain core factors such as protein distribution/placement or the existence of elements which is still essential to understand the parts in play for cell-to-cell communication. Therefore, it is beneficial to analyse the whole cell to combine the measurement of electrochemical techniques with imaging techniques (Yoo et al., 1990). Which are essentially covering the lacking areas required in analysis, as viewing inside the cells avoids false positives. With confocal imaging, both outside and inside the cell can be analysed. As PIP2 is known on the plasma membrane for actin dynamics, exocytosis, and endocytosis, inside images of the cell should be explored to avoid false positives. Confocal microscope has the ability to focus diffraction-limited spots in samples, rejecting out-of-focus light from the image (Elliott, 2020; Nwaneshiudu, et al., 2012). Allowing specific images of cell sections throughout the cell and more precise analysis of cell placement/distribution on factors inside cells (Elliott, 2020; Nwaneshiudu, et al., 2012).

This project aims to analyse the position of PIP2, to study if it exists on the membrane of LDCV and analyse the possible effect the lipid has on LDCV. The analysis is accomplished by using confocal imaging for localization, as it discloses both the outside and inside of the cells. PLC $\delta$ 1 and NPY-mCherry makes PIP2 and LDCV fluorescent, respectively. VIEC amperometry is used for directly examining the fusion kinetics of the vesicles. These methods will be using PC12, and bovine chromaffin cells, respectively, as the former is more accessible to culture and prepare for imaging, and the second yields more vesicles for amperometry analysis (Lovell et al., 2000; Liu et al., 1999).

## **Materials and methods**

### **Imaging – Confocal**

#### **PC12 Cells**

PC12 cells were maintained at 37°C/5% CO<sub>2</sub> in RPMI 1640 (Life Technologies) in modified DMEM containing DMEM (500 U/ml) (Life Technologies), Glutmax (5 U/ml) (Life Technologies), Horse serum (25 U/ml) (Life Technologies), FCS (25 U/ml) (Life Technologies), PIS (5 U/ml) (Life Technologies), HEPES (5 U/ml) (Life Technologies), Sodium Pyruvate (5 U/ml) (Life Technologies) and Mercia (0.5 U/ml) (Life Technologies). Cells were plated on Poly-D-Lysine (Life Technologies) coated coverslips and transfected with fluorescent marker using lipofectamine 2000 (Invitrogen) in Opti-mem (Life Technologies). Imaging was performed 24 to 48 hours after transfection. PC12 cells were provided as a kind gift from Robert Fredriksson, Department of Pharmaceutical Biosciences in Uppsala, originating from ATCC.

#### **Plasmids and Solutions**

PIP2 is detected by using PLC $\delta$ 1 (0.5 ng/ $\mu$ L), provided by Olof Idevall-Hagren (Omar-Hmeadi et al., 2018). Granule markers used are NPY-mCherry (0.4 ng/ $\mu$ L) (Gandasi et al., 2015). Both reagents were stored at 4 °. Cells were imaged in an extracellular solution containing NaCl (138 mM), KCl (5.6 mM),

MgCl<sub>2</sub> (1.2 mM), CaCl<sub>2</sub> (2.6 mM), 3 D-glucose, and 5 HEPES with the adjusted PH 7.4 with NaOH. All experiments were carried out at 37°C.

## **Microscopy**

The cell samples are studied with confocal microscopy, performed by a Zeiss LSM700 microscope with a confocal 63x/1.40 objective (Zeiss). Sequential scanning consists of a red channel (excitation 555 nm) and a green channel (excitation 488 nm). The size of the pinhole is 0.61  $\mu$ M, corresponding to 1 Airy unit. Images were acquired in 16-bit at gain settings 750 for both channels and 0.4  $\mu$ M per pixel. Each image consists mostly of a singular cell on which image analysis is performed upon.

## **Image Analysis**

Confocal images were opened and analysed in Fiji Software ImageJ 1.53c (Wayne Rasband, National Institutes of Health, U.S.A.). Analysis consisted of picking quality images of cells plasma membrane and cytoplasm regions in which both transfections were clearly visible. Thereafter, the images for PIP2 is firstly analysed for cluster density with given macro "find maxima for granule density" (Gandasi et al., 2015). These are thereafter compared with their corresponding image for NPY-mCherry if they are not control samples.

## **Statistics**

These experiments were repeated with at least four independent preparations each, for control and sample study. Data is presented as mean  $\pm$  standard deviation when required. Statistical significance was assessed using Students t-test for unpaired samples as to discern if there is a difference in the two groups as the t-test is a standard parametric test for studying differences in means and drawing comparison in large quantity data.

## **Amperometric Analysis**

### **Bovine Chromaffin Cell**

Chromaffin cells are acquired through fresh Bovine adrenal glands, kindly donated by Dalsjöfors Kött AB, Dalsjöfors, Sweden. The glands are kept in Lockes buffer (1x) before vesicle extraction. Lockes buffer (10 $\times$ , pH 7.4) containing 1.54 M NaCl, 56 mM KCl, 36 mM NaHCO<sub>3</sub>, 56 mM glucose, and 50 mM HEPES was diluted by distilled water each time to obtain the 1 $\times$  Lockes buffer for storage and rinsing the adrenal glands.

### **Vesicle Isolation**

Bovine adrenal glands are cleaned off fat, lipids and rinsed off blood/waste with homogenizer buffer (310 mOsm/kg) contained 0.3 M sucrose, 1 mM EDTA, 1 mM MgSO<sub>4</sub>, 10 mM HEPES, 10 mM KCl, and complete Protease Inhibitor (Roche, Sweden). Once cleaned, glands were separated in the middle and had the medulla region extracted and placed in homogenizer buffer. Extracted chromaffin cells are placed in a homogenization buffer and crushed at a speed of 1000 rpm with a Homogenizer and a Potter-Elvehjem PTFE pestle with glass tube. Chromaffin pieces are directly placed in a centrifuge set

at 1000g, 10 min, 4.0 °C. The supernatant is kept and centrifuged again at 10000g, 20 min, 4 °C. Discard the supernatant and add 10 ml homogenization buffer. The vesicle sample is kept at 4°C and used within 24 hours.

### **Addition of PIP2**

BODIPY FL phosphatidylinositol 4,5-biphosphate, (300 uM) (Echelon Biosciences) combined with Histone H1 Carrier (100 uM) (Echelon Biosciences) was incubated for 10 minutes after vigorous pipetting to facilitate complex formation. Further diluted in a ratio of 1:10 with homogenization buffer. The prepared complex was added along with homogenization buffer and prepared vesicle sample together in a 1:3 ratio and put in 4 °C 12 hours before testing.

### **Carbon Fiber Electrode Fabrication**

Carbon Fiber Electrodes (C.F.E.s) were created with the combination of 33-um diameter C.F.E. was located into a borosilicate capillary (10cm length, O.D: 1.2mm, I.D: 0.69mm., Sutter Instrument Co., Novato, CA, U.S.A.) through aspiration. Micropipette puller (Model P-1000, Sutter Instrument Co., Novato, CA, U.S.A.) was used to melt and pull each capillary creating tips. The capillary tips are sealed through epoxy (Epoxy Technology, Billerica, MA, U.S.A.). After, All electrodes were kept at 100°C for 24 hours for hardening, subsequently cut at the glass junction and bevelled at a 45° angle on the tip with a beveller (EG-400, Narishige Inc., London, U.K.). Prior to each electrochemical experiment, each electrode went through testing of cyclic voltammetry in a standard dopamine solution (100uM) in PBS pH 7.4 (-0.2 to 0.8 V vs Ag/AgCl, at scan rate 100 mV/s), C.F.E. of acceptable steady state were used.

### **Vesicle Impact Electrochemical Cytometry**

Electrochemical detection of single isolated vesicle content was performed on C.F.E. surface at a constant potential of +700 mV/ Ag-AgCl operated by a potentiostat (Axopatch 200B, Molecular Devices). Electrode was placed in in vesicle solution with exposed surfaced aimed upwards. Each analysis was carried out with at least, 5 to 10 min depending on the number of peaks acquired.

### **Amperometric Analysis**

Amperometric signals were converted in Matlab software (The MathWorks, Inc.) and analysed with IgorPro software (Wavemetrics, Lake Oswego, OR). A binomial filter and the detection limit was set to 1 kHz and five times the standard deviation of the noise measured as the threshold for peak detection. Also, all amperometric traces were checked manually and after peak detection, the false positives were manually removed. Each spike as a representative of one vesicle was analysed using Faraday's law ( $N=Q/nF$ ), where  $Q$  is the area under the peak,  $N$ , number of catecholamine molecules, obtained by integrating the area under the peak,  $F$  is Faraday's constant and  $n$  is the number of electrons produced during the oxidation reaction ( $n=2$  for catecholamines) (Larsson., 2019). Also, each spike was analysed by the following parameters at figure 11.  $I_{max}$  (pA), the peak current intensity,  $t_{rise}$  (ms), rise time, defined as the time that takes for the current to increase from 25% to 75% of  $I_{max}$ ,  $t_{1/2}$  (ms), the half peak width at half-maximum  $I_{max}$ ,  $t_{fall}$  (ms), fall time, defined as the time that takes for the current to drop from 75% to 25% of  $I_{max}$ .

## Statistics

These experiments were repeated with at least two independent preparations each. Each practice yielded ten attempts to perform VIEC analysis, in total twenty VIEC analyses each for control and sample group. Data is presented as mean  $\pm$  standard deviation when required. Statistical significance was assessed using a Student's t-test for unpaired samples as to discern if there is a difference in the two groups as the t-test is a standard parametric test for studying differences in means and drawing comparison in large quantity data.

## Results

### Imaging Results

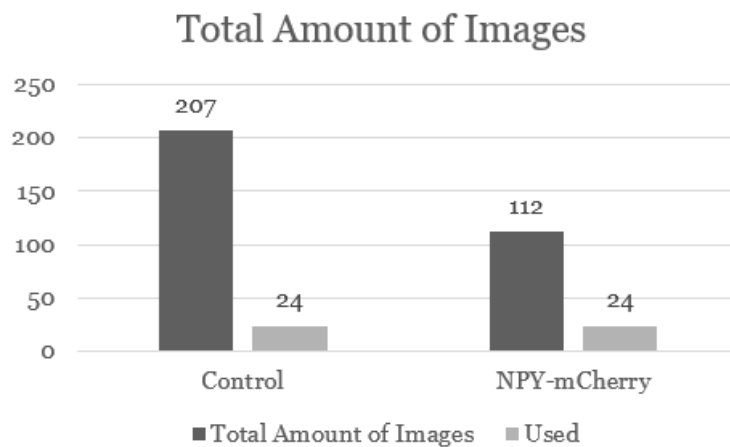


Figure 1. Figure of the number of confocal images taken of both control (n=207) and NPY-mCherry (n=112). 24 images of each group were picked based on quality and used for co-localization analysis (n=24 images for each group).

To study the location PIP2, PIP2 marker PLC $\delta$ 1 tagged to EGFP was co-transfected with granule markers label NPY-mCherry, then imaged using confocal microscopy. In total, 207 control confocal images were taken on PC12 the cell plasma membrane and cytoplasm section, and 112 confocal images similar images were taken on PC12 cells transfected with PLC $\delta$ 1 and granule marker NPY-mCherry as seen in Figure 1. Plasma membrane and cytoplasm section images were taken to discern the localization of clusters found. 24 of the best images were used in both groups to quantify peaks in fluorescence spots.



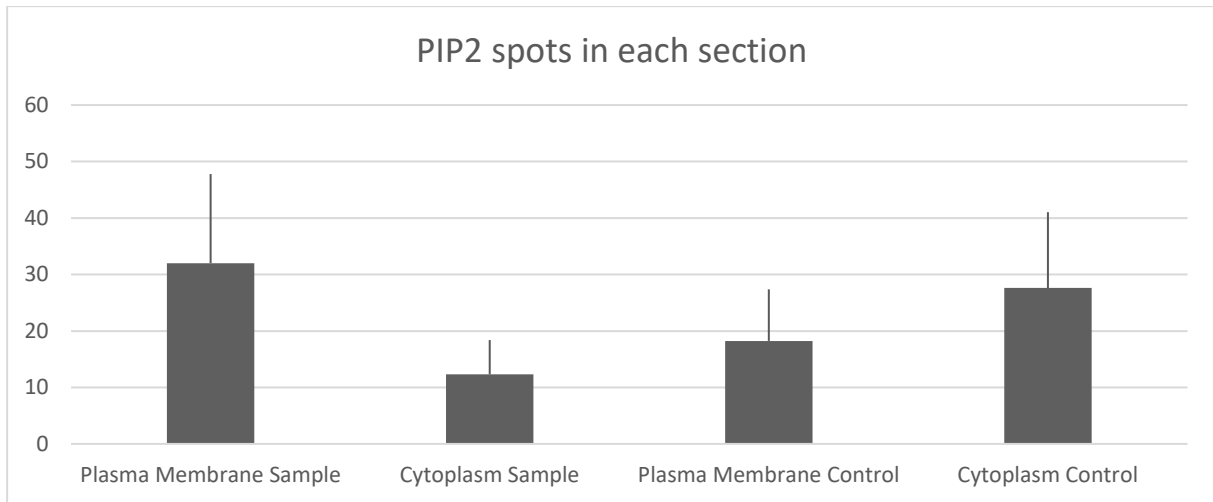


Figure 2. Figure indicating the range of spots on each cell for each section on PC12 cells, PM (Plasma membrane), CP (Cytoplasm) (PM sample, 32, std 15.78. CP Sample 12.32, std 6.07. PM Control 18.24, std 9.13. CP Control 27.6, std 13.43).

The number of clusters between images and area is not consistent, especially seen with cytoplasm sample consisting of overall fewer than other groups. However, although an inequality of clusters, the overlapping still shows an apparent similarity in the image analysis between the two markers, showcasing similar points of high-density fluorescent in individual spots in both sections.

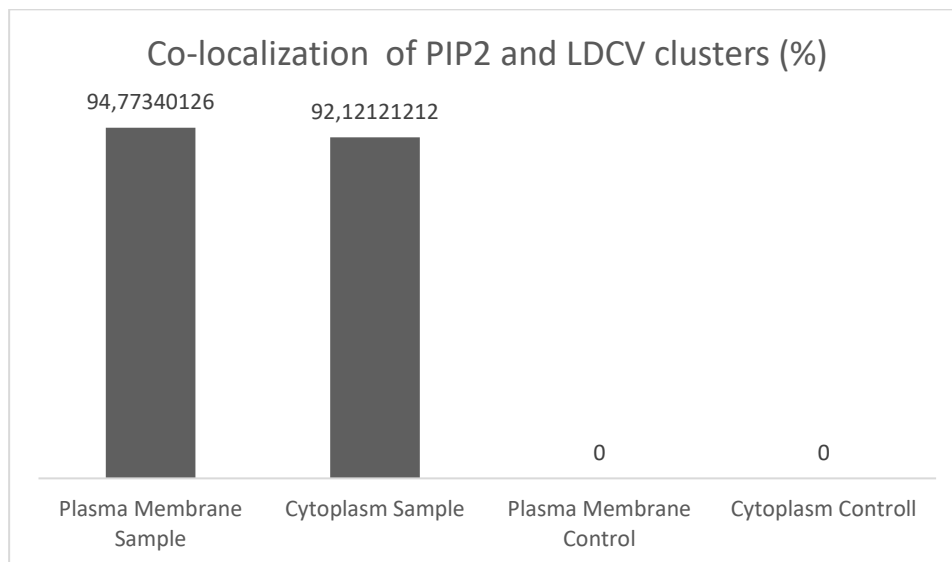


Figure 3. Figure indicating %, Co-localization of plasma membrane/cytoplasm sample shows a substantial similarity between locations, meaning that PIP2 and LDCV share placement and PIP2 is on the LDCV membrane. The values of zero on the control group are because there is no comparison to be drawn.

Comparison of the clusters between the two fluorescence groups indicate over 90% similarity. With plasma membrane section yielding 94.773% and Cytoplasm 92.121%, as seen in Figure 3. Clusters which do not overlap could be due to overexposure which would be missed in analytical procedure.

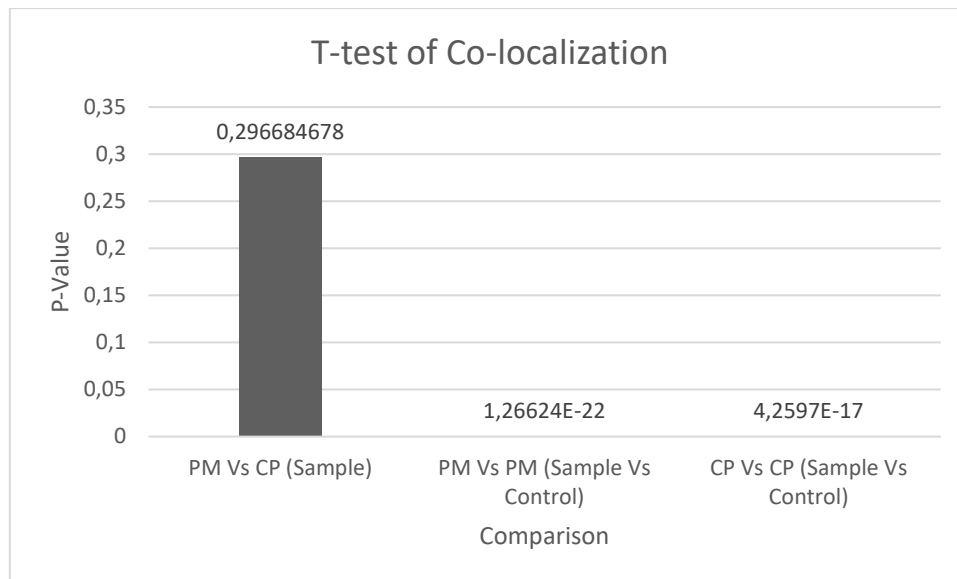


Figure 4 indicates that there is no significant difference between the spots in the plasma membrane and cytoplasm regions of cells transfected with NPY-mCherry and PLC $\delta$ 1 ( $P < 0.296$ ), while also showing a clear significance between NPY-mCherry/PLC $\delta$ 1 with the plasma membrane ( $P < 1.266E-22$ ) and cytoplasm ( $P < 4.259E-17$ ).

Figure showcases student t-test results, which compares the significance spots difference between sample/sample, sample/control and control. Only between the plasma membrane sample and cytoplasm sample does there not exist a difference with the use of t-test. Indicating placement of PIP2 on LDCV. Comparative to the other control groups/regions in which t-test strongly indicate significant difference.

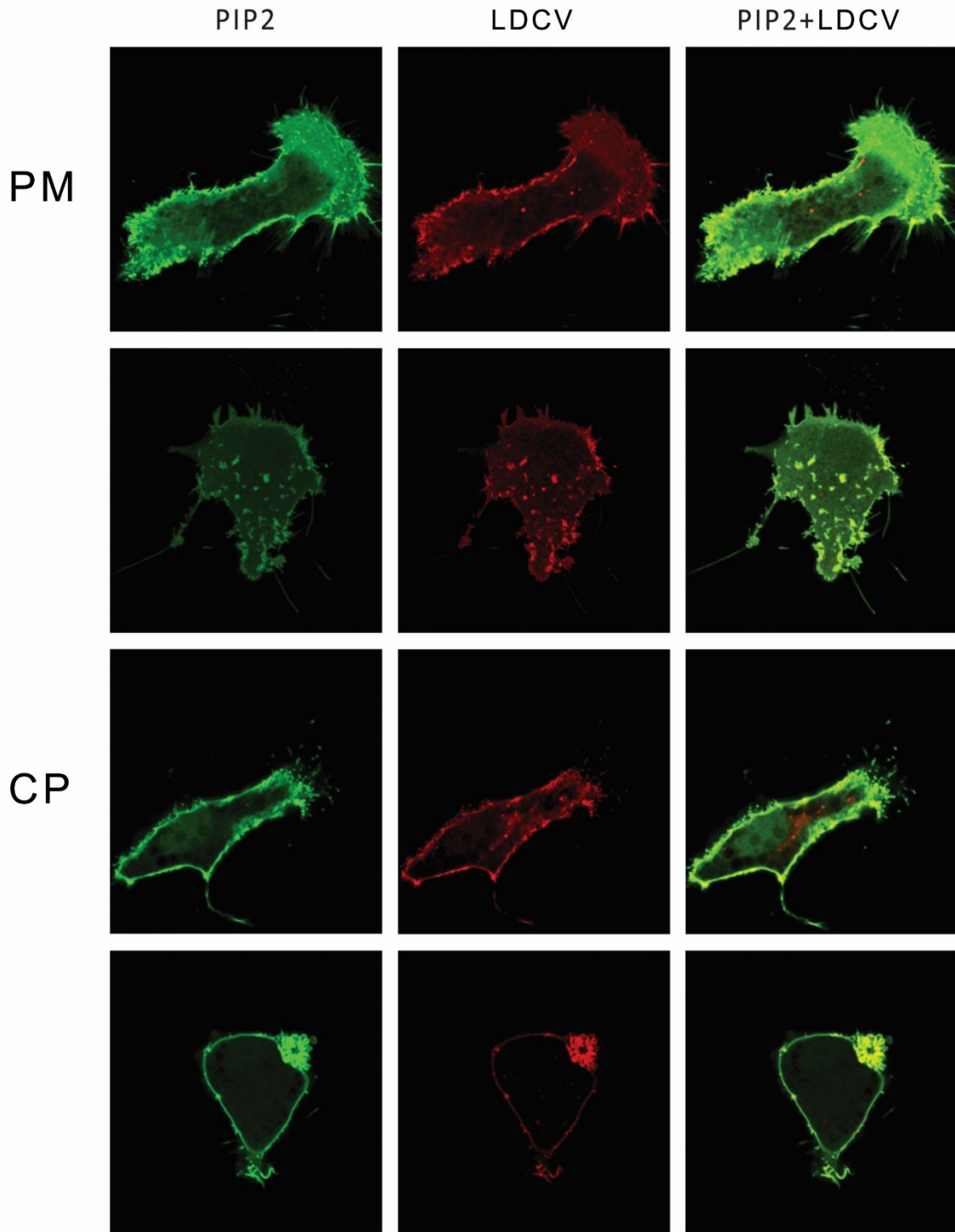


Figure 5. Confocal Imaging of only PIP2, only granules, and combined. Cells transfected with NPY-mCherry and PLC $\delta$ 1 indicate a similar position of lipid PIP2 and LDCV. Plasma membrane (PM) and Cytoplasm (CP) section images display clear nanodomains of PIP2 in clear visible spots overlapped with LDCV. They show the placement of overlapping high-concentration points of both markers. Certain areas in the midsection display NPY-mCherry markers with a bit of marking of PIP2, but high fluorescent spots exist near the membrane or directly on the membrane.

Examples of retrieved images are shown in Figure 5, illustrating the placement of PIP2 and LDCV on PC12 cells. Overall strong similarity between both PIP2 and LDCV across the images. With individual regions specifically at the cytoplasm not having overlapping of both targets.

## Vesicle Impact Electrochemical Cytometry Results

To analyse the possible effect of PIP2 has on the LDCV membrane, a total of twenty samples for each group (sample and control) was analysed. VIEC amperometric resulted in no significant difference in the parameters apart from half-time ( $P < 0.0938$ ), as seen in figure 6a-e.

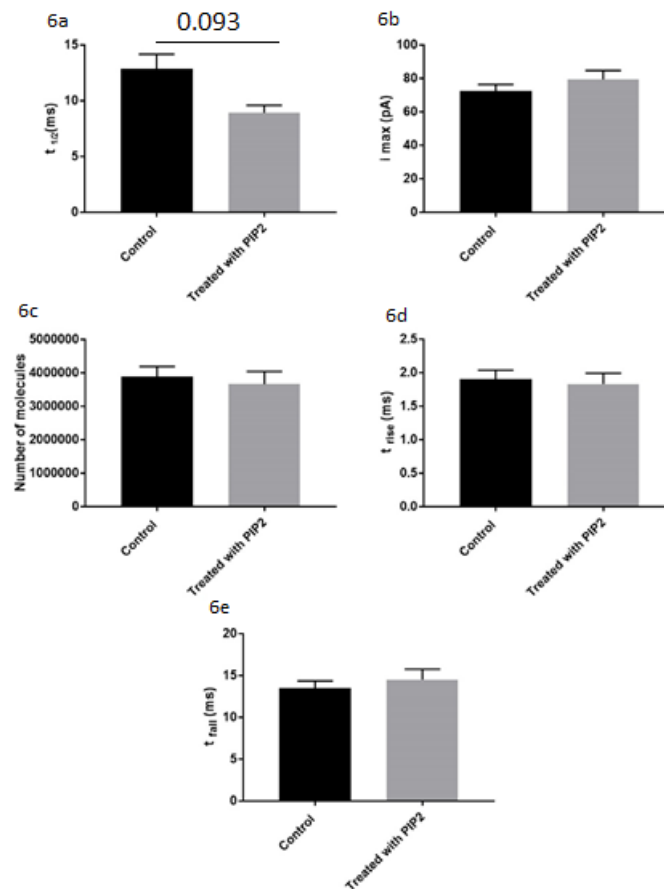


Figure 6a-e. (n=20) Student t-tests of VIEC parameters between control vesicles and treated with PIP2. Figure 6a. Figure of Half time ( $t_{1/2}$  ms) between control vesicles and treated with PIP2. Difference is significant ( $P < 0.0938$ ). Figure 6b. Figure of  $I_{max}$  (pA) between control and treated with PIP2. Difference is not significant ( $P < 0.4778$ ). Figure 6c. Figure of number of molecules in control and treated with PIP2. Difference is not significant ( $P < 0.6586$ ). Figure 6d. Figure of  $t_{rise}$  (ms) in control and treated with PIP2. Difference is not significant ( $P < 0.3862$ ). Figure 6e. Figure of  $t_{fall}$  in control and treated with PIP2. Difference is not significant ( $P < 0.8738$ ).

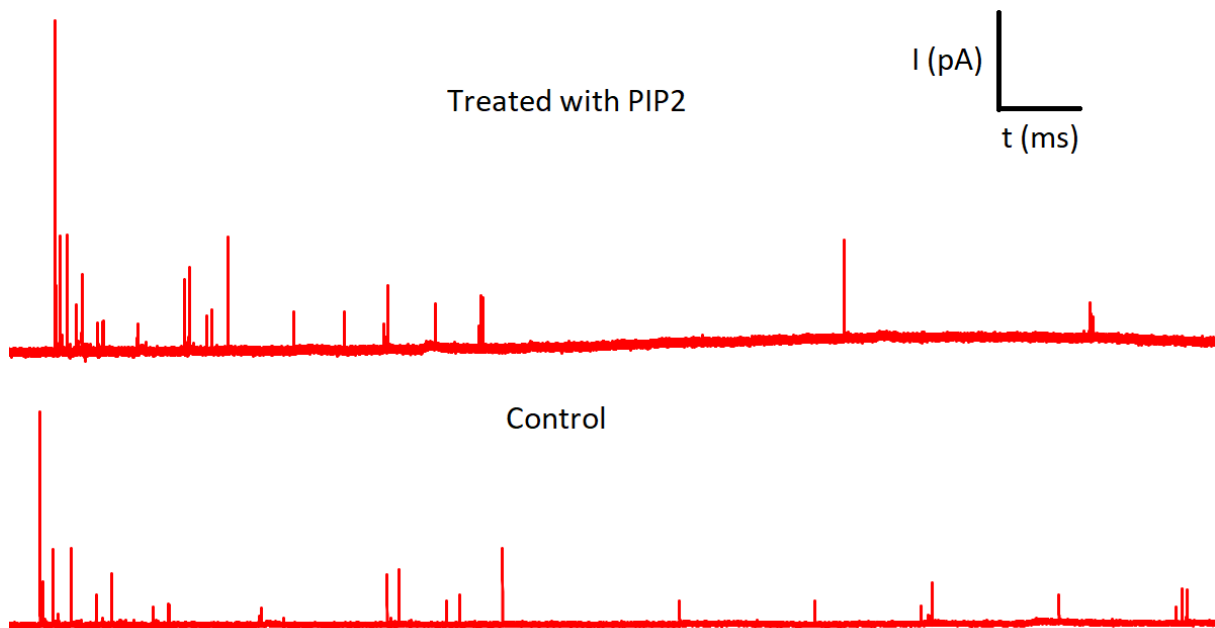


Figure 7. Figure showcasing amperometric traces of 24 hours old control vesicles and treated retrieved from VIEC.

Amperometric traces, result of LDCV bursting at contact with the CFE, result in peaks based on neurotransmitters oxidating after exposure. Figure 7 showcases example of both groups where multiple peaks have occurred over time. Different sizes of the peaks are determined by the amount of neurotransmitters in each LDCV. In which, based on the potential, the amount of neurotransmitters can be calculated through the use of Faraday's Law,  $N_{molecules} = N_A Q / nF$ . Average trace reside at 5-10 min which is based on the amount of traces acquired. Due to CFE placement, CFE quality and quality of LDCV, more time may be required for LDCV to collide with the CFE.

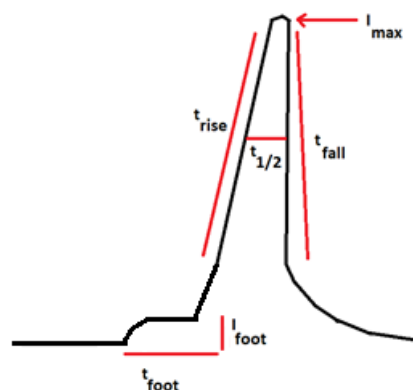


Figure 8. The figure shows amperometric peaks, which conclude a bursting vesicle and the parameters. These parameters consist of  $t_{foot}$ ,  $I_{foot}$ ,  $t_{1/2}$ ,  $t_{rise}$ ,  $t_{fall}$ , and  $I_{max}$ .  $t_{foot}$  and  $I_{foot}$  studies specifically for vesicles release at cell membrane and is hence not analysed here.

Each individual peak used in this analysis follow these parameters. Representing the bursting of a LDCV and content (neurotransmitters) oxidizing causing change in action potential. Numerous peaks are retrieved during analysis, in which multitude can be caused by noise which are exempted from the study. Based on previous finding in figure 6a, the half time was decreased which represents the overall

duration of the exocytotic phase. No other parameter such as closing and opening was noticeable on their own.  $I_{\text{foot}}$  and  $t_{\text{foot}}$  are not accounted in this study, due to analysing free vesicles, which  $I_{\text{foot}}/t_{\text{foot}}$  analyse vesicles opening at the cell membrane before the whole peak comes to by the oxidated neurotransmitters.

## Discussion

In this study, 24 quality confocal images of PC12 cells transfected with NPY-mCherry and PLC $\delta$ 1 (Figure 1) indicate that PIP2 is like LDCV in confocal Imaging regarding placement. Several images with examples in figure 5 show clusters displaying significant fluorescent overlap on both markers for PIP2 and LDCV on the same cell. These essential markers on the plasma membrane are mainly allocated to high fluorescent areas clearly shown on the membrane. It is with most importance to discern the precise location of both markers, as PIP2 is already known on the cell membrane, membrane which LDCV are drawn towards for, risking false positives (Dembla & Becherer., 2021). These domains are showcased at a lesser frequency at the mid-section of the cell with varying placements, presumably due to decreased membrane area. Most positions of the clusters are allocated to concentrated spots in the direct vicinity of the membrane. With NPY-mCherry marker, extending a bit away from the membrane, with overlapping PLC $\delta$ 1 marker. With two markers consistently overlapping with a 90% co-localization, as seen in figure 3, it strongly suggests the placement of PIP2 is indeed on the membrane of LDCV. This 90% co-localization is still due even to the shifting total of clusters between sections, presumably due to the quality of images and the difference in cells. Student t-test used to compare difference in clusters on the different regions of the cell indicates no significant difference between the sample group spots percentage compared to control. The difference in total spots between sections is fault by practice during lab procedure, presumably caused by overexposure to fluorescent markers during imaging. Even with a difference in total clusters, the difference seemingly did not affect the co-localization percentage.

Analysis of VIEC amperometry (figure 6a-6e) revealed that the only significance to a certain degree, ( $P < 0.0938$ ) added PIP2 had on LDCV is on the half-time parameter ( $t_{1/2}$ ) and no other form of parameters. Other parameters, represented at figure 8, such as  $t_{\text{rise}}$ ,  $t_{\text{fall}}$ , number of molecules, and  $I_{\text{max}}$  represent the time to open, time to close, total neurotransmitters in the vesicle, and maximum current, respectively (Larsson, 2019). Half-time in primary represents the entire duration of the exocytotic phase at the exocytosis process, but in the VIEC, it indicates the period of vesicle opening (bursting) (Larsson, 2019). In this case, the faster half-time represents the LDCV membrane breaking up quicker than control group. This change accompanied by the unaffected parameters could presume that PIP2 accumulation destabilizes the membrane further, which results in a quicker opening when in contact with the C.F.E. But due to this study being observational at the base, no direct conclusion can be made to the source of the effect, apart from simple findings and discussions. Such as the analysis not being on a cell, these functions which occurred on the LDCV membrane must be passive in nature. The elevated concentration of PIP2 could result in larger nanodomains that caused membrane conformation change, which could be the cause for decreased half time, resulting in quicker opening. PIP2, previously shown to accumulate in nanodomains at the membrane (Bilkova et al., 2017; Sarmiento et al., 2014). When binding in clusters, the headgroup of the lipid changes angle practically parallel to the membrane (Kishore. & Prestegard., 2003). As discussed at length by Borges-Araújo and Fernandes (2020), the accumulation of PIP2 clusters through their molecular interactions, the

headgroup angle likely influences the acyl-chain dynamics, affecting membrane order. Such assemblies are also argued by Borges-Araújo and Fernandes (2020) to be causing downstream signalling of PIP2 likely. And perhaps could be the reason for the decrease in half-time, due to the LDCV inability to react upon added PIP2 levels, compared to a cell.

The techniques in this article were of great use to perform observational analysis. The combination yielded both placement and effect of said placement. The individual procedures use different kinds of cells to analyse, adapted for their use. PC12 cells ease culture, and Bovine chromaffin cells large vesicles supply enough specimens to examine. Both methods have the quality to acquire precise results and are quick to perform, which lowers the time needed for analysis. Although VIEC may be susceptible to noise or ill-quality peaks, such as the result of either poor equipment handling or production of the C.F.E. With C.F.E. being the most demanding with its room for mistake, the tip can easily be broken or exposed, yielding peaks unusable due to noise. The combined analysis of Imaging and Amperometry is an excellent observational tool combined due to this. PC12 cells are argued to be unsuitable for comment due to the nature of cancer cells due to affected metabolism (DeBerardinis & Chandel., 2016). But as an observational analysis, and it works as an analytical cell.

The findings could further understand the PIP2 part in cell-to-cell communication and LDCV. Added PIP2 levels presumably enhance the release of LDCV cargo which promotes it more for a suitable target for future medicine. To either enhance or decrease PIP2 levels directly affect LDCV fusion kinetics for a deeper purpose. Such as affecting norepinephrine and epinephrine, amongst other targets. If membrane instability results from accumulating PIP2 levels, certain disorders may be caused due to an inability to handle increased PIP2 levels, which damages cells directly. This study has indicated the placement of PIP2 on LDCV and that their effect is significant on half-time, presumably having a direct impact on overall membrane stability. They resulted in a faster breakdown for LDCV. Results were acquired in this article with confocal imaging and VIEC amperometry analysis. This discovery adds more to PIP2 in effect and placement and lays a possible ground for further analysing PIP2 direct part in LDCV fusion kinetics. As well as enhance the combined use of both techniques for future studies regarding other biological targets.

In conclusion, this work studied and found the lipid PIP2 to be placed on the membrane of LDCV with the use of confocal microscopy and fluorescence markers. As well concluded on the effect PIP2 has on the vesicles with VIEC amperometric, indicating to decrease membrane stability, presumably due to formation of nano cluster domains. Both showing significant through t-test analysis. This finding may serve helpful for future studies regarding cell-to-cell communication with LDCV or PIP2. This effect may also serve as a therapeutic target to affect LDCV regarding different kinds of disease and conditions. This study also serves to indicate the useability of both combining Imaging techniques and electrochemical analysis.

## **Acknowledgments**

For this article I wish to thank Nikhil and Amir for the great support and aid which they provided during the whole procedure. As well for Shakar Said and Neha Sinha for aiding me with confocal usage. I also

thank Novonordisk Fonden for supporting with chemicals. As well Robert Fredriksson for providing PC12 cells.

## Reference

Bader, M. F., Holz, R. W., Kumakura, K., & Vitale, N. (2002). Exocytosis: the chromaffin cell as a model system. *Annals of the New York Academy of Sciences*, 971, 178–183. <https://doi.org/10.1111/j.1749-6632.2002.tb04461.x>

Bilkova, E., Pleskot, R., Rissanen, S., Sun, S., Czogalla, A., Cwiklik, L., Róg, T., Vattulainen, I., Cremer, P. S., Jungwirth, P., & Coskun, Ü. (2017). Calcium Directly Regulates Phosphatidylinositol 4,5-Bisphosphate Headgroup Conformation and Recognition. *Journal of the American Chemical Society*, 139(11), 4019–4024. <https://doi.org/10.1021/jacs.6b11760>

Borges-Araújo, L., & Fernandes, F. (2020). Structure and Lateral Organization of Phosphatidylinositol 4,5-bisphosphate. *Molecules (Basel, Switzerland)*, 25(17), 3885. <https://doi.org/10.3390/molecules25173885>

Chen, T. K., Luo, G., & Ewing, A. G. (1994). Amperometric monitoring of stimulated catecholamine release from rat pheochromocytoma (PC12) cells at the zeptomole level. *Analytical chemistry*, 66(19), 3031–3035. <https://doi.org/10.1021/ac00091a007>

DeBerardinis, R. J., & Chandel, N. S. (2016). Fundamentals of cancer metabolism. *Science advances*, 2(5), e1600200. <https://doi.org/10.1126/sciadv.1600200>

Dembla, E., & Becherer, U. (2021). Biogenesis of large dense core vesicles in mouse chromaffin cells. *Traffic (Copenhagen, Denmark)*, 22(3), 78–93. <https://doi.org/10.1111/tra.12783>

Elliott A. D. (2020). Confocal Microscopy: Principles and Modern Practices. *Current protocols in cytometry*, 92(1), e68. <https://doi.org/10.1002/cpcy.68>

Gandasi, N. R., Vestö, K., Helou, M., Yin, P., Saras, J., & Barg, S. (2015). Survey of Red Fluorescence Proteins as Markers for Secretory Granule Exocytosis. *PloS one*, 10(6), e0127801. <https://doi.org/10.1371/journal.pone.0127801>

Greene, L. A., & Tischler, A. S. (1976). Establishment of a noradrenergic clonal line of rat adrenal pheochromocytoma cells which respond to nerve growth factor. *Proceedings of the National Academy of Sciences of the United States of America*, 73(7), 2424–2428. <https://doi.org/10.1073/pnas.73.7.2424>

Grishanin, R. N., Kowalchuk, J. A., Klenchin, V. A., Ann, K., Earles, C. A., Chapman, E. R., Gerona, R. R., & Martin, T. F. (2004). CAPS acts at a pre-fusion step in dense-core vesicle exocytosis as a PIP2 binding protein. *Neuron*, 43(4), 551–562. <https://doi.org/10.1016/j.neuron.2004.07.028>

Hay, J. C., Fiset, P. L., Jenkins, G. H., Fukami, K., Takenawa, T., Anderson, R. A., & Martin, T. F. (1995). ATP-dependent inositide phosphorylation required for Ca(2+)-activated secretion. *Nature*, 374(6518), 173–177. <https://doi.org/10.1038/374173a0>



- Kabachinski, G., Yamaga, M., Kielar-Grevstad, D. M., Bruinsma, S., & Martin, T. F. (2014). CAPS and Munc13 utilize distinct PIP2-linked mechanisms to promote vesicle exocytosis. *Molecular biology of the cell*, 25(4), 508–521. <https://doi.org/10.1091/mbc.E12-11-0829>
- Kishore, A. I., & Prestegard, J. H. (2003). Molecular orientation and conformation of phosphatidylinositides in membrane mimetics using variable angle sample spinning (VASS) N.M.R. *Biophysical journal*, 85(6), 3848–3857. [https://doi.org/10.1016/S0006-3495\(03\)74799-7](https://doi.org/10.1016/S0006-3495(03)74799-7)
- Larsson, A. (2019). *Electrochemical and Microscopic Analysis of Chemical Signalling in Biological Systems*. [Doktorsavhandling, Göteborgs Universitets]
- Liu, M., Dunn, P. M., King, B. F., & Burnstock, G. (1999). Rat chromaffin cells lack P2X receptors while those of the guinea-pig express a P2X receptor with novel pharmacology. *British journal of pharmacology*, 128(1), 61–68. <https://doi.org/10.1038/sj.bjp.0702790>
- Lovell, P. V., James, D. G., & McCobb, D. P. (2000). Bovine versus rat adrenal chromaffin cells: big differences in B.K. potassium channel properties. *Journal of neurophysiology*, 83(6), 3277–3286. <https://doi.org/10.1152/jn.2000.83.6.3277>
- Mandal K. (2020). Review of PIP2 in Cellular Signaling, Functions and Diseases. *International journal of molecular sciences*, 21(21), 8342. <https://doi.org/10.3390/ijms21218342>
- Martin T. F. (2012). Role of P.I. (4,5)P(2) in vesicle exocytosis and membrane fusion. *Sub-cellular biochemistry*, 59, 111–130. [https://doi.org/10.1007/978-94-007-3015-1\\_4](https://doi.org/10.1007/978-94-007-3015-1_4)
- Montesinos, M. S., Machado, J. D., Camacho, M., Diaz, J., Morales, Y. G., Alvarez de la Rosa, D., Carmona, E., Castañeyra, A., Viveros, O. H., O'Connor, D. T., Mahata, S. K., & Borges, R. (2008). The crucial role of chromogranins in storage and exocytosis revealed using chromaffin cells from chromogranin A null mouse. *The Journal of neuroscience : the official journal of the Society for Neuroscience*, 28(13), 3350–3358. <https://doi.org/10.1523/JNEUROSCI.5292-07.2008>
- Nwaneshiudu, A., Kuschal, C., Sakamoto, F. H., Anderson, R. R., Schwarzenberger, K., & Young, R. C. (2012). Introduction to confocal microscopy. *The Journal of investigative dermatology*, 132(12), e3. <https://doi.org/10.1038/jid.2012.429>
- Omar-Hmeadi, M, Gandasi, NR, Barg, S. PIP2 is not required for secretory granule docking. *Traffic*, 19, 436–445. <https://doi.org/10.1111/tra.12562>
- Sarmiento, M. J., Coutinho, A., Fedorov, A., Prieto, M., & Fernandes, F. (2014). Ca(2+) induces PI(4,5)P2 clusters on lipid bilayers at physiological PI(4,5)P2 and Ca(2+) concentrations. *Biochimica et biophysica acta*, 1838(3), 822–830. <https://doi.org/10.1016/j.bbamem.2013.11.020>
- Tuosto, L., Capuano, C., Muscolini, M., Santoni, A., & Galandrini, R. (2015). The multifaceted role of PIP2 in leukocyte biology. *Cellular and molecular life sciences : CMLS*, 72(23), 4461–4474. <https://doi.org/10.1007/s00018-015-2013-0>
- Westerink, R. H., & Ewing, A. G. (2008). The PC12 cell as model for neurosecretion. *Acta physiologica (Oxford, England)*, 192(2), 273–285. <https://doi.org/10.1111/j.1748-1716.2007.01805.x>

Yoo, S. H., Albanesi, J. P., & Jameson, D. M. (1990). Fluorescence studies of nucleotide interactions with bovine adrenal chromogranin. *A. Biochimica et biophysica acta*, 1040(1), 66–70. [https://doi.org/10.1016/0167-4838\(90\)90146-7](https://doi.org/10.1016/0167-4838(90)90146-7)